



Pergamon

Bioorganic & Medicinal Chemistry Letters 12 (2002) 1559–1562

BIOORGANIC &
MEDICINAL
CHEMISTRY
LETTERS

Synthesis and Pharmacological Characterization of a Potent, Orally Active p38 Kinase Inhibitor

Jacques Dumas,^{a,*} Holia Hatoum-Mokdad,^a Robert N. Sibley,^a Roger A. Smith,^a William J. Scott,^a Uday Khire,^a Wendy Lee,^a Jill Wood,^a Donald Wolanin,^a Jeffrey Cooley,^a Donald Bankston,^a Aniko M. Redman,^a Robert Schoenleber,^a Yolanda Caringal,^a David Gunn,^a Romulo Romero,^a Martin Osterhout,^a Holger Paulsen,^a Timothy J. Housley,^b Scott M. Wilhelm,^b John Pirro,^c Du-Shieng Chien,^c Gerald E. Ranges,^b Alka Shrikhande,^b Andrew Muzsi,^b Elizabeth Bortolon,^b Jean Wakefield,^b Cynthia Gianpaolo Ostravage,^b Ajay Bhargava^b and Thuy Chau^b

^aDepartment of Chemistry Research, Bayer Research Center, 400 Morgan Lane, West Haven, CT 06516, USA

^bDepartment of Cancer and Osteoporosis Research, Bayer Research Center, 400 Morgan Lane, West Haven, CT 06516, USA

^cInstitute of Preclinical Drug Development, Bayer Research Center, 400 Morgan Lane, West Haven, CT 06516, USA

Received 26 March 2002; accepted 16 April 2002

Abstract—Inhibitors of the MAP kinase p38 provide a novel approach for the treatment of osteoporosis, inflammatory disorders, and cancer. We have identified *N*-(3-*tert*-butyl-1-methyl-5-pyrazolyl)-*N'*-(4-(4-pyridinylmethyl)phenyl)urea as a potent and selective p38 kinase inhibitor in biochemical and cellular assays. This compound is orally active in two acute models of cytokine release (TNF-induced IL-6 and LPS-induced TNF) and a chronic model of arthritis (20-day murine collagen-induced arthritis). © 2002 Elsevier Science Ltd. All rights reserved.

The MAP kinase p38 is involved in IL-1 β and TNF α signaling pathways,¹ and provides a novel approach to the treatment of osteoporosis and inflammatory disorders. For example, SB 203580 (**1**, Fig. 1), shows potent activity in models of endotoxin shock and bone resorption.² In addition, p38 kinase has been linked to angiogenesis through cellular VEGF production.³ Screening of a Bayer combinatorial chemistry library afforded a novel class of p38 inhibitors such as urea **2**.

Early optimization of urea **2** (Fig. 1) into phenylpyrazolyl ureas has already been reported in this journal, and provided in vivo proof-of-principle for this compound class.⁴ More recently, X-ray crystallographic data suggested that diarylureas are binding to an allosteric domain of p38 kinase.⁵ The present report focuses on optimization of phenoxy-phenyl urea **3**, resulting in

further improvements of both potency and drug-like properties.⁶

Synthetic routes to ureas similar to **2** and **3**, as well as the SAR of the pyrazole unit of urea **2** have already been reported by our group.^{4,7} The focus of this study is the bisaryl ether side chain of **3** (Tables 1 and 2). While the introduction of nonpolar substituents at the 4-position of

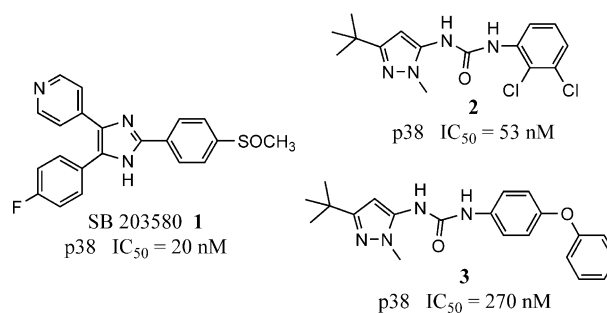


Figure 1. P38 kinase inhibitors.

*Corresponding author. Tel.: +1-203-812-5204; fax: +1-203-812-3655; e-mail: jacques.dumas.b@bayer.com

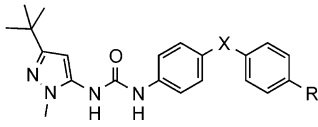
the phenoxy group (entries **4–6**) does not seem to impact p38 kinase activity, addition of hydrogen bond donors such as amides (**7–9**), carbamates (**11–12**), or phenols (**13**) improves potency. Pyridines **22** and **23** (Table 2) also offer good replacements for the phenyl group of **3** and display potent activity in both the p38 kinase assay and the functional assay (IL-1–TNF α -induced IL-6 production in SW1353 cells).⁸ The oxygen linker atom of urea **3** can easily be replaced by a sulfur atom, a methylene, or a thiomethylene group. The observation that the length of the linker is non-critical for activity, and that hydrophilic substituents are preferred on this side of the molecule suggests that the extremity of the biaryl side chain could be extending into solvent. Our first acute in vivo model measures TNF α induced IL-6 production in mice, and provides oral efficacy data with a rapid turnaround time.⁹ Carbamate **11** shows a promising in vitro profile, but does not demonstrate significant activity in our in vivo screening model (Table 3). In contrast, urea **23** and its

methylene analogue **22** show significant effects in this model, at doses ranging from 25 to 50 mg/kg po. The latter analogue was selected for chronic pharmacology studies.

The in vitro kinase selectivity of urea **22** was evaluated against a panel of receptor kinases and cytosolic kinases. Of these, only the isoform p38 β 1 is inhibited at appreciable levels.¹⁰ This finding appears consistent with the hypothesis developed by Regan et al.⁵ in which pyrazolyl ureas bind to an allosteric site specific to p38, outside of the ATP pocket. Plasma exposure following single dose oral administration in mice was then measured, and is depicted in Figure 2. Micromolar levels of **22** are maintained for 4 h after a 10 mg/kg single oral administration (0.5% Tween 80/water vehicle). The ability of urea **22** to block LPS-induced TNF α synthesis¹¹ was also measured, and is summarized in Table 4. Potent inhibition of TNF α production is observed at 20 mg/kg po single dose. In comparison, SB 203580 **1** is also efficacious in this model (30 mg/kg po).

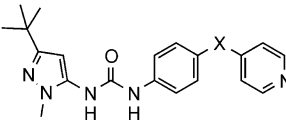
The activity of urea **22** was then assessed in a 20-day, murine model of arthritis (Fig. 3, Table 5).¹² In this model, mice are immunized with bovine type II collagen, then treated with test compounds or vehicle. The onset of arthritis is then measured using a variety of parameters, including a clinical score, and three histopathology readouts. Both compounds **1** and **22** showed oral efficacy in this model at 50 and 30 mg/kg po daily dose, respectively.

Table 1. Substitution of the bisaryl ether



Compd	X	R	p38 α 2 (IC ₅₀ , nM)	SW1353 (IC ₅₀ , nM)
3	O	H	270	
4	O	CH ₃	160	
5	O	<i>tert</i> -Bu	183	
6	O	OCH ₂ Ph	110	
7	O	NHCOCH ₃	235	
8	O	NHCOCH ₂ CH(CH ₃) ₂	45	313
9	O	NHCOCH ₂ CH ₃	69	1060
10	O	NH ₂	310	
11	O	NHCO ₂ Et	33	87
12	O	NHCO ₂ -iPr	54	162
13	S	OH	35	1100
14	S	OnPr	57	235
15	S	OnBu	69	>2500
16	CH ₂	NHCOCH ₂ CH(CH ₃) ₂	37	170
17	CH ₂	NHCO ₂ - <i>tert</i> -Bu	87	57
18	CH ₂	NH ₂	290	
19	CH ₂	NHCOCH ₃	70	
20	CH ₂	NHCOCH ₂ CH ₃	38	1750
21	CH ₂	NHCO(CH ₂) ₂ CO ₂ H	200	>2500

Table 2. Substitution of the bisaryl ether: linker atom



Compd	X	p38 α 2 (IC ₅₀ , nM)	SW1353 (IC ₅₀ , nM)
22	CH ₂	42	323
23	S	13	95
24	SCH ₂	140	
25	CH ₂ S	44	584
26	NH	420	
27	CH ₂ CH ₂	430	
28	OCH ₂	260	

Table 3. Activity of selected analogues in TNF α -induced IL-6 short-term in vivo model

Compd	Aqueous solubility (mg/L)		Dose (mg/kg po)	% Inhib.	<i>p</i> Value
	pH 7.5	pH 2.0			
1			100	80	0.001
22	50	2000	50	84	0.003
22			25	60	0.01
23	655	1658	100	90	<0.001
23			50	77	<0.001
11	95	77	50	16	NS
25	322	5155	50	64	<0.001
25			25	22	0.025
25			10	–15	NS

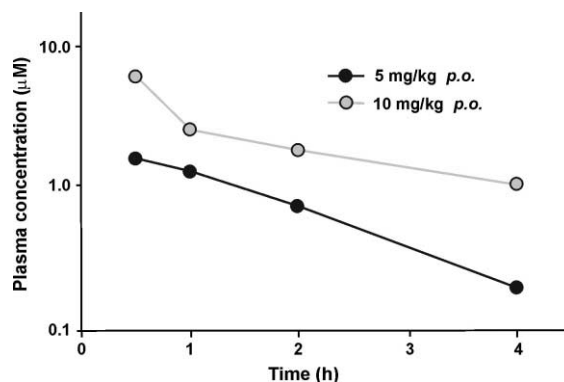
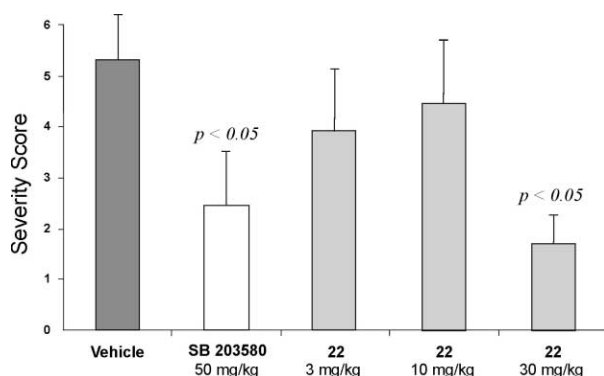


Figure 2. Plasma exposure of urea **22**, following a single-dose oral administration in mice.

Table 4. Activity of compounds **1** and **22** in LPS-induced TNF α production in mice

Compd	Dose (mg/kg po)	Plasma TNF α (ng/mL, \pm SEM)	% Inhib.	<i>p</i> Value
Vehicle		37.5 \pm 2.9		
1	10	38.0 \pm 5.6	–1.4	NS
1	30	13.0 \pm 2.8	65.4	<0.0001
22	10	46.7 \pm 5.3	–24.5	NS
22	20	19.8 \pm 2.3	47.1	<0.0001
22	50	5.1 \pm 0.7	86.5	<0.0001

**Figure 3.** Activity of SB 203580 (**1**) and urea **22** in 20-day murine collagen-induced arthritis model: severity scores.

In conclusion, optimization of urea **3** through a combined combinatorial and medicinal chemistry effort resulted in improvements of both potency and drug-like properties. As a result, we identified *N*-(3-*tert*-butyl-1-methyl-5-pyrazolyl)-*N'*-(4-(4-pyridinyl-methyl)phenyl)urea **22**¹³ as a potent and selective inhibitor of the MAP kinase p38. This analogue is orally available in mice, and shows significant *in vivo* activity in two acute models of cytokine release (TNF α -induced IL-6 and LPS-induced TNF α) and a chronic model of arthritis (20-day murine collagen induced arthritis).

Acknowledgements

We would like to thank Christopher Browe, Tim Sarr, and Robert Dreyer (cloning and purification of p38 α 2 kinase and MKK-6), and Teresa Lopes (solubility measurements) for their support. We are also grateful to Charles Maniglia, David Brittelli, Timothy Lowinger, Bernd Riedl, and Robert Carlson for helpful discussions.

References and Notes

- Gallagher, T. F.; Fier-Thompson, S. M.; Garigipati, R. S.; Sorenson, M. E.; Smietana, J. M.; Lee, D.; Bender, P. E.; Lee, J. C.; Laydon, J. T.; Chabot-Fletcher, M. C.; Breton, J. J.; Adams, J. L. *Bioorg. Med. Chem. Lett.* **1995**, *5*, 1171.
- Badger, A. M.; Bradbeer, J. N.; Votta, B.; Lee, J. C.; Adams, J. L.; Griswold, D. E. *J. Pharm. Exper. Ther.* **1996**, *279*, 1453.
- Yamamoto, T.; Kozawa, O.; Tanabe, K.; Akamatsu, S.; Matsuno, H.; Dohi, S.; Uematsu, T. *J. Cell. Biochem.* **2001**,

Table 5. Activity of SB 203580 (**1**) and urea **22** in 20-day murine collagen-induced arthritis model: clinical scores and histopathology

Compd	Dose (mg/kg)	Clinical score	Histopathology	
		No. paws affected	% regression	IC IO
Vehicle		2.3 \pm 0.4	19.1 \pm 8.0	1.13 0.63
1	50	1.0 \pm 0.4 ^a	65.0 \pm 13.5 ^a	0.63 ^a 0.25 ^a
22	3	1.4 \pm 0.5	43.5 \pm 15.8	0.80 0.33
22	10	1.9 \pm 0.5	25.0 \pm 13.4	0.78 0.30
22	30	0.7 \pm 0.3 ^a	61.7 \pm 14.5 ^a	0.38 ^a 0.20 ^a

IC, inflammatory cells; IO, interstitial oedema.

^aSignificant from vehicle ($p < 0.05$).

82, 591. Jackson, J. R.; Bolognese, B.; Hillegass, L.; Kassis, S.; Adams, J.; Griswold, D. E.; Winkler, J. D. *J. Pharmacol. Exper. Ther.* **1998**, *284*, 687.

4. Dumas, J.; Sibley, R.; Riedl, B.; Monahan, M.-K.; Lee, W.; Lowinger, T. B.; Redman, A. M.; Johnson, J. S.; Kingery-Wood, J.; Scott, W. J.; Smith, R. A.; Bobko, M.; Schoenleber, R.; Ranges, G. E.; Housley, T. J.; Bhargava, A.; Wilhelm, S. M.; Shrikhande, A. *Bioorg. Med. Chem. Lett.* **2000**, *10*, 2047. Ranges, G. E.; Bortolon, E.; Chau, T.; Dixon, B. R.; Bhargava, A.; Dumas, J.; Gianpaolo-Ostravage, C.; Hatoum-Mokdad, H.; Housley, T. J.; Shrikhande, A.; Scott, W. J.; Sibley, R.; Wakefield, J.; Wilhelm, S. M. 220th ACS National Meeting, Washington, DC, Aug 20–24, 2000; MEDI-149.

5. Pargellis, C.; Tong, L.; Churchill, L.; Cirillo, P. F.; Gilmore, T.; Graham, A. G.; Grob, P. M.; Hickey, E. R.; Moss, N.; Pav, S.; Regan, J. *Nat. Struct. Biol.* **2002**, *9*, 268.

6. Dumas, J.; Hatoum-Mokdad, H.; Sibley, R.; Smith, R. A.; Scott, W. J.; Khire, U.; Lee, W.; Wood, J.; Wolanin, D.; Cooley, J.; Bankston, D.; Redman, A.; Schoenleber, R.; Caringal, Y.; Housley, T. J.; Wilhelm, S. M.; Pirro, J.; Chien, D. S.; Ranges, G. E.; Shrikhande, A.; Muzsi, A.; Bortolon, E.; Wakefield, J.; Gianpaolo-Ostravage, C.; Chau, T. 222nd ACS National Meeting, Chicago, IL, Aug 26–30, 2001; MEDI-256.

7. Redman, A. M.; Johnson, J. S.; Dally, R.; Swartz, S.; Wild, H.; Paulsen, H.; Caringal, Y.; Gunn, D.; Renick, J.; Osterhout, M.; Kingery-Wood, J.; Smith, R. A.; Lee, W.; Dumas, J.; Wilhelm, S. M.; Housley, T. J.; Bhargava, A.; Ranges, G. E.; Shrikhande, A.; Young, D.; Bombara, M.; Scott, W. J. *Bioorg. Med. Chem. Lett.* **2001**, *11*, 9.

8. *P38 kinase in vitro assay*: purified and His-tagged p38 α 2 (expressed in *Escherichia coli*) was activated in vitro by MMK-6 to a high specific activity. Using a microtiter format, all reactions were conducted in 100 μ L volumes with reagents diluted to yield 0.05 μ g/well of activated p38 α 2 and 10 μ g/well of myelin basic protein in assay buffer (25 mM HEPES 7.4, 20 mM MgCl₂, 150 mM NaCl). Test compounds (5 μ L of a 10% DMSO solution in water) were prepared and diluted into the assay to cover a final concentration range from 5 nM to 2.5 μ M. The kinase assay was initiated by addition of 25 μ L of an ATP cocktail to give a final concentration of 10 μ M cold ATP and 0.2 μ Ci [γ -³³P] ATP per well (200–400 dpm/pmol of ATP). The plate was incubated at 32 $^{\circ}$ C for 35 min, and the reaction quenched with 7 μ L of a 1 N aq HCl solution. The samples were harvested onto a P30 Filtermat (Wallac, Inc.) using a TomTec 1295 Harvester (Wallac, Inc.), and counted in a LKB 1205 Betaplate Liquid Scintillation Counter (Wallac, Inc.). Negative controls included substrate plus ATP alone. *SW1353 cellular assay*: SW1353 cells (human chondro-sarcoma, ATCC, Bethesda, MD) are seeded (1000 cells/100 μ L DMEM 10% FCS/well) into 96-well plates and incubated overnight. After medium replacement, cells are exposed to test compounds for 1 h at 37 $^{\circ}$ C, at which time human IL-1 (1 ng/mL, Endogen, Woburn, WA) and recombinant human TNF α (10 ng/mL) are added. Cultures are incubated for 48 h at

37 °C, then supernatant IL-6 values are determined by ELISA (Endogen, Woburn, WA). For both assays, at least two independent IC₅₀ determinations were performed on each compound, and the mean value is reported. SB203580 (**1**) was used as a standard (p38 IC₅₀ = 20 nM, SW1353 IC₅₀ = 50 nM). In all cases, standard deviations were less than 50% of the mean IC₅₀ value.

9. *In vivo* IL-6 induction by TNF α : BALB/c female mice are dosed po with test compounds and given an ip injection of rHuTNF after 1 h. Two hours later, animals are bled by cardiac puncture. Plasma IL-6 levels are determined by ELISA, SB 203580 (**1**) is used as a positive control.

10. *In vitro* kinase selectivity of urea **22**: this data was obtained in house and at MDS Panlabs (Bothell, WA):

p38 α 2	IC ₅₀ = 42 nM
p38 β 1	IC ₅₀ = 110 nM
HER-2	IC ₅₀ = 4.2 μ M
JNK-1	2% inhibition at 0.5 μ M
ERK-1	8% inhibition at 5 μ M
abl	3% inhibition at 5 μ M
p59 ^{lck}	8% inhibition at 10 μ M
p59 ^{fyn}	20% inhibition at 10 μ M
PKA	7% inhibition at 10 μ M
PKC α	0% inhibition at 10 μ M
PKC β	5% inhibition at 10 μ M
PKC γ	21% inhibition at 10 μ M
EGFR	17% inhibition at 10 μ M

11. *In vivo* TNF α induction by LPS: Female BALB/c mice are dosed po with test compounds (0.5% Tween 80/water vehicle). After 1 h, animals are treated with 100 μ g LPS (ip injection). After 90 min, the animals are bled by cardiac puncture. TNF α levels in plasma are determined by ELISA, SB 203580 (**1**) is used as a positive control.

12. *Murine collagen induced arthritis in vivo model*: this model was performed at Chrysalis International, Inc. On day 0, groups of 12 mice are immunized at the base of the tail with 100 μ g of bovine type II collagen, which is emulsified with complete Freund's adjuvant. On day 7, a second booster dose of collagen is administered the same way. On day 14, the mice are treated with 100 μ g LPS (sc). On day 21, at the onset of arthritis, the mice are dosed po once daily with test compounds or vehicle (0.5% Tween 80 in water) for 20 days. Paw oedema is measured by a constant caliper, and arthritic manifestations are clinically scored during the 20-day observation period. The severity score is the total clinical score (rated from 0 to 4 for each paw) divided by the total number of mice in the group. Column 'No. paws affected' reflects the total number of affected paws divided by the number of mice in the group. At the end of the study, the paws are removed and examined histologically (number of inflammatory cells, interstitial oedema). Positive control dexamethasone (3 mg/kg po) totally prevents the onset of arthritis in this model.

13. Large scale preparation of urea **22**: Step 1: Synthesis of 5-amino-3-*tert*-butyl-1-methylpyrazole. A solution of pivaloyl-acetonitrile (320 g, 2.56 mol) in ethanol (3000 mL) was treated with methylhydrazine (180 mL, 155.88 g, 3.38 mol), and the contents were heated to 70 °C for 18 h. The solution was then cooled to room temperature and concentrated to a white solid, which was triturated with hexane (2 \times 2000 mL) to provide 5-amino-3-*tert*-butyl-1-methylpyrazole (373 g, 2.43 mol, 95%) as colorless needles after vacuum drying. ¹H NMR (CDCl₃) δ 1.26 (s, 9H, *tert*-butyl), 3.45 (br s, 2H, -NH₂), 3.63 (s, 3H, -NCH₃), 5.42 (s, 1H, -CH). Anal. calcd for C₈H₁₅N₃: C, 62.71; H, 9.87; N, 27.42. Found: C, 62.80; H, 9.66; N, 27.35. MS/EI: *m/z* 153 (M⁺); 138 (M-CH₃).

Step 2: Synthesis of 4-(4-pyridinylmethyl)benzenamine. A mixture of 4-(4-nitrophenylmethyl)pyridine (200.0 g, 933.62 mmol) and 10% Pd/C (34 g, Degussa type) in 1000 mL of ethanol/ethyl acetate (4:1) was shaken in a Parr vessel under 20–30 psi hydrogen pressure until reduction was complete by TLC detection. The mixture was filtered over Celite, and the filtrate was concentrated. The solids were triturated with hot 20% ethanol/hexane (1000 mL) to provide 4-(4-aminophenylmethyl)pyridine (165.0 g, 895.57 mmol, 96%) as a light-brown solid after vacuum drying. ¹H NMR (DMSO-*d*₆) δ 3.74 (s, 2H, -CH₂-), 4.92 (br s, 2H, -NH₂), 6.49, 6.87 (AA'BB', *J* = 8.4 Hz, 4H, phenyl), 7.17, 8.41 (AA'BB', *J* = 5.9 Hz, 4H, phenyl). Anal. calcd for C₁₂H₁₂N₂: C, 78.23; H, 6.57; N, 15.20. Found: C, 77.94; H, 6.41; N, 15.15. MS/EI: *m/z* 184 (M⁺). Mp 156–158 °C.

Step 3: synthesis of urea **22**. A suspension of 5-amino-3-*tert*-butyl-1-methylpyrazole (300.0 g, 1.96 mol) in methylene chloride (3000 mL) was treated with CDI (334.0 g, 2.06 mol, 1.05 equiv) in one portion, and the mixture was stirred at room temperature under argon. After 15 min, dissolution occurred, and the temperature of the solution slowly rose to 30 °C. After 60 min, the reaction flask was charged with 4-(4-aminophenylmethyl)pyridine (361.10 g, 1.96 mol) in one portion, and the internal temperature slowly rose to a gentle reflux. When the internal temperature cooled to 36 °C, the contents were stirred for 18 h at that temperature under an atmosphere of argon. The reaction mixture was then cooled to room temperature, washed with brine (3 \times 2000 mL) and the organic phase was dried (sodium sulfate) and concentrated to a tan solid foam. The crude product was heated to reflux in ethyl acetate (4000 mL) for 20 min, cooled to 30 °C and treated with diethyl ether (4000 mL). Suction filtration provided *N*-(3-*tert*-butyl-1-methyl-5-pyrazolyl)-*N'*-(4-(4-pyridinylmethyl)phenyl)urea **22** (601.0 g, 1.65 mol, 84%) as a pale-yellow solid. ¹H NMR (DMSO-*d*₆) δ 1.19 (s, 9H, *t*-butyl), 3.57 (s, 3H, -NCH₃), 3.88 (s, 2H, -CH₂-), 6.02 (s, 1H, -CH), 7.14, 7.38 (AA'BB', 8.5 Hz, 4H, Ph), 7.21, 8.44 (AA'BB', 5.9 Hz, 4H, phenyl), 8.43 (s, 1H, -NH), 8.82 (s, 1H, -NH). MS/FAB: *m/z* 364 (M+1). Anal. calcd for C₂₁H₂₅N₅O: C, 69.40; H, 6.93; N, 19.27. Found: C, 69.04; H, 6.93; N, 19.34. Mp 161–162 °C.